ABUAD Journal of Engineering Research and Development (AJERD)
ISSN (online): 2645-2685; ISSN (print): 2756-6811

Volume 8, Issue 1, 129-139

Synthesis of Multi-Walled Carbon Nanotubes Modified Rutile (TiO_2/MWCNTs) Composite for Photocatalytic Degradation of Textile Wastewater

Tunmise Latifat ADEWOYE[1], Omowumi Mardiyah ISSA[1], Ishaq Alhassan MOHAMMED[1], Sherif Ishola MUSTAPHA[1,3], Omodele Abiodun Abosede ELETTA[1], Fatai Alade ADERIBIGBE[1], Saka Ambali ABDULKAREEM[2]

[1]*Department of Chemical Engineering, University of Ilorin, PMB 1515 Ilorin, Kwara Nigeria*
adewoye.tl@unilorin.edu.ng/omowumiisa@gmail.com/mohammed.ia@unilorin.edu.ng/Mustapha.si@unilorin.edu.ng/modeletta@unilorin.edu.ng/aderibigbe.fa@unilorin.edu.ng

[2]*Department of Chemical Engineering, Federal University of Technology, PMB 65 Minna, Niger State, Nigeria*
kasaka2003@futminna.edu.ng

[3]*School of Chemical and Metallurgical Engineering, University of the Witwatersrand, Private Bag X3, P O BOX 2050, South Africa*
sherif.mustapha@wits.ac.za

Corresponding Author: adewoye.tl@unilorin.edu.ng, +2348032170062
Date Submitted: 18/08/2024
Date Accepted: 13/02/2025
Date Published: 15/02/2025

Abstract*: Photocatalysis has emerged as a sustainable and efficient approach for the treatment of industrial wastewater, offering the potential to degrade persistent organic pollutants under light irradiation. This study explores the enhanced photocatalytic degradation of textile wastewater using a TiO_2-based nanocomposite photocatalyst. The composite was synthesized by modifying rutile TiO_2, derived from natural rutile ore, with multi-walled carbon nanotubes (MWCNTs) through a hydrothermal process. The microstructure, morphology, chemical composition, surface area, and phase structure of rutile-TiO_2, MWCNTs, and the TiO_2/MWCNTs nanocomposite were characterized using different characterization techniques including high-resolution transmission electron microscopy (HRTEM), high-resolution scanning electron microscopy (HRSEM), UV-Vis spectroscopy, Brunauer-Emmett-Teller (BET) surface area analysis, and X-ray diffraction (XRD). Photocatalytic activity was evaluated by measuring the degradation of organic pollutants, with chemical oxygen demand (COD) and phenol concentration as indicators, under both artificial and natural sunlight irradiations. The results revealed that the incorporation of MWCNTs significantly enhanced the photocatalytic performance of rutile TiO_2. Under visible light, phenol removal efficiencies were 59% and 42% for the TiO_2/MWCNTs nanocomposite and rutile-TiO_2, respectively, while under sunlight, the removal rates increased to 73% and 56%. Similarly, COD reduction was 55% for TiO_2/MWCNTs compared to 35% for rutile-TiO_2 under visible light, and 73% versus 56% under sunlight. These findings demonstrate that MWCNT modification improves the photoactivity of rutile-TiO_2, offering a cost-effective and sustainable approach to wastewater treatment using photocatalysts derived from natural ore. This study presents a viable alternative for synthesizing TiO_2-based materials for environmental remediation.*

Keywords: *Rutile, Photocatalyst, Hydrothermal, Nanocomposite, Textile, Phenol*

1. INTRODUCTION

Environmental pollution remains a critical global challenge, with industries contributing significantly to the contamination of water bodies through the release of untreated effluents [1, 2]. Industrial activities such as textile production, mining, smelting, electroplating, and printing generate wastewater containing highly toxic pollutants that are discharged into the environment at alarming rates [3-6]. Global wastewater generation in 2020 was estimated at 359 billion cubic meters (m^3) and is projected to rise to 470 billion m^3 by 2030, reaching approximately 574 billion m^3 by 2050 [3]. The textile industry, while essential for economic development, poses significant environmental threats through the discharge of dye-laden wastewater [7, 8]. The presence of dyes in water reduces light penetration, inhibits photosynthetic activity, and depletes dissolved oxygen, adversely affecting aquatic ecosystems [9, 10]. Additionally, untreated wastewater introduces high levels of organic pollutants, including chemical oxygen demand (COD), biological oxygen demand (BOD), and total organic carbon (TOC), leading to severe water quality degradation [11, 12]. To mitigate these environmental and health risks, various conventional wastewater treatment methods have been developed, such as adsorption, coagulation, ion exchange, membrane filtration, and oxidation processes [13, 14]. However, these methods often have limitations, including high costs, incomplete removal of pollutants, and the generation of secondary waste.

Among advanced treatment technologies, heterogeneous photocatalysis using titanium dioxide (TiO_2) has garnered significant attention for its efficiency, cost-effectiveness, and environmental compatibility [15, 16]. TiO_2 exhibits remarkable properties, including long-term photostability, chemical inertness, and the ability to oxidize organic and inorganic pollutants under ambient conditions. Moreover, it operates effectively under solar irradiation, further enhancing its appeal as a sustainable treatment option [17]. TiO_2 exists in three polymorphic forms which include anatase, rutile, and brookite with anatase and rutile being the most prominent for photocatalytic applications due to their respective bandgap energies of 3.2 eV and 3.0 eV [18]. Although anatase has been extensively studied, growing interest has shifted towards the rutile phase and its potential for photocatalysis [19]. Typically, rutile-TiO_2 is synthesized in laboratories using chemical precursors, but natural rutile ore offers a cost-effective alternative for producing TiO_2, as demonstrated by Yilleng et al. [19]. Despite its advantages, the photocatalytic efficiency of TiO_2 is constrained by its limited absorption of visible light and the rapid recombination of electron (e-) –hole (h+) pairs [20]. Enhancing TiO_2's activity under visible light has driven researchers to explore modifications such as doping, co-doping, composite formulations, and coupling with other materials, including metals and non-metals [12].

Multi-walled carbon nanotubes (MWCNTs) are particularly promising modifiers due to their exceptional mechanical strength, large surface area, excellent electronic properties, and chemical stability [21]. Incorporating MWCNTs into TiO_2 composites enhances UV photoactivity and modifies surface properties, enabling visible light sensitivity, as demonstrated by Shaari & Mohamed [17]. Researchers have successfully synthesized TiO_2/MWCNT composites using anatase-TiO_2 for dye degradation [21, 22]. However, limited studies have explored the photocatalytic performance of rutile-TiO_2/MWCNTs nanocomposites for the simultaneous degradation of phenol and COD in real textile wastewater under visible and natural sunlight irradiation.

This study aims to address this gap by synthesizing rutile-TiO_2/MWCNTs nanocomposites from natural rutile ore. The photocatalytic performance of these composites will be compared with bare rutile-TiO_2 to evaluate their efficacy in degrading textile wastewater and to investigate the kinetics of the photocatalytic degradation process.

2. MATERIALS AND METHODS

2.1 Collection of Samples

All the reagents used for experimental studies are of analytical grade (98-99.7%) and do not require further purification. Concentrated hydrochloric acid (HCl), concentrated nitric acid, HNO_3, and ethanol were obtained from Sigma Aldrich. Rutile ore was used as the precursor for TiO_2. The rutile sample employed in this work was obtained from the North Eastern part (Bauchi State) of Nigeria. The rutile sample was collected, cleaned, and pulverised according to the method described by Yilleng et al. [19], while the textile wastewater sample was obtained from a textile industry in Kaduna, Kaduna State in North Western part of Nigeria. The Wastewater was collected in a sterilized plastic container and kept in the refrigerator at 4˚C.

2.2 Synthesis and Purification of MWCNTs

The MWCNTs were synthesized using the method described in Adewoye et al. [23] with slight modification. The MWCNTs were synthesized at the temperature of 750°C for 45 min in a CVD reactor at an acetylene flow rate of 100 mL/min and an argon flow rate of 200 mL/min. The synthesized MWCNTs were purified by dispersing 2.0 g of MWCNTs in 100 mL aqua regia [24]. The solution was stirred in a beaker and sonicated for 3 h at 45°C to remove impurities and to create oxygenated functional groups on the nanotube's surface. The MWCNTs were then filtered and washed thoroughly with distilled water until a neutral pH was achieved. The MWCNTs were dried at 105°C in an oven. The obtained purified MWCNT sample was kept in an airtight container at room temperature before use.

2.3 Preparation of Rutile-TiO_2/MWCNTs

The rutile-TiO_2/MWCNTs nanocomposite was prepared using the hydrothermal method. Rutile-TiO_2 was used as a titanium source. 0.01- 0.05 g of the treated MWCNTs were each introduced into a flask containing 1 g of rutile in a mixture of deionized water (10 mL) and ethanol (25 mL). The obtained mixture was sonicated for 15 min. The resulting solution was separated by centrifuging for 20 min at 4000 rpm. Next, the wet rutile-TiO_2/MWCNTs composite obtained was dispersed in 200 mL of a deionized water/ethanol mixture (1:1 v/v), and placed in a Teflon-lined stainless-steel reactor (autoclave) and thermally treated at 120 °C for 4 h. After that, the obtained precipitate was allowed to cool to room temperature and the resulting powdered mixture was filtered, washed with deionized water several times, and dried in an oven at 110 °C for 2 h [25]. The final product was kept in a sterile sample bottle for subsequent use.

2.4 Characterization of MWCNT, Rutile and Rutile-TiO2/MWCNTs

The phase structure and the crystallite size of MWCNTs, rutile, and rutile-TiO_2/ MWCNTs were investigated by (XRD) model Bruker AXS D8 with CuKα radiation. HRSEM was used to investigate the morphological characterization of MWCNTs, rutile-TiO_2, and rutile-TiO_2/MWCNTs. HRTEM analysis was performed for size measurement and microstructure. The specific surface areas of the samples were determined by N_2 adsorption at 77 K by the (BET) method (NOVA 4200e, Quantachrome Instruments, USA). The optical absorption and band gap spectra of rutile-TiO_2, rutile-TiO_2/MWCNTs nanocomposite, and MWCNTs were measured by a UV-vis spectrophotometer (UV-1800 Series) in the range of 280–800 nm.

2.5 Textile Wastewater Characterization

The chemical and physical properties of raw textile dyeing wastewater sample, with special emphasis on (BOD), (COD), phenol content, colour absorbance, and total dissolved solids (TDS) were carried out.

2.6 Photocatalytic Degradation of Textile Wastewater

The degradation of textile wastewater under artificial and natural solar irradiation was used to test the photocatalytic performance of rutile-TiO_2 and synthesized rutile-TiO_2/MWCNTs photocatalyst. The photocatalytic performance was evaluated by the degradation of phenol and COD as the target pollutants. Irradiation tests were carried out in a batch-mode photocatalytic reactor (with a space in the upper section for sampling and a UV lamp) that was kept at a constant temperature by a water jacket. The light source was a low-pressure mercury bulb. The reactor set-up was covered with a wooden box to prevent the light from leaking. For each run, 0.5 g of rutile-TiO_2/MWCNTs composite powder was dispersed in a beaker containing 50 mL of textile wastewater. The mixture was stirred in the dark for 60 min to reach adsorption/desorption equilibrium, and then UV light radiation was used to degrade the phenol and COD. The first sample was taken just before the lamp was turned on, at the end of dark adsorption. The textile effluent was then exposed to UV light while being stirred at a constant speed. After 150 min of irradiation, the degradation activity ceased. Samples were periodically drawn from the vessel, Whatman filters (PTFE-membrane, 0.45 μm) were used to filter all samples to remove catalyst particles, and the filtrate was analysed for their phenol and COD content. This method was replicated under sunlight as an irradiation source. The percentage removal of pollutants was calculated by using the (Equation 1) [26]:

$$R = \frac{(C_o - C_t)}{Co} \text{ x } 100\% \quad (1)$$

where C_o is the initial concentration of pollutant (phenol or COD) solution and C_t is the final concentration of pollutants (phenol or COD)

3. RESULTS AND DISCUSSION

3.1 Characterisation of the Developed Materials

3.1.1 X-ray diffraction analysis of rutile-TiO_2, MWCNTs and rutile-TiO_2/MWCNTs

The phase and crystallinity of MWCNTs, rutile-TiO_2/MWCNTs (5 weight% MWCNTs), and rutile-TiO_2 were analysed through XRD diffraction patterns and presented in Figure 1. The XRD pattern of MWCNTs exhibits two main peaks at 26.4° and 44. 6° corresponding to the (002) and (100) diffraction plane of MWCNTs in agreement with Taha et al.., 2022[27]. The peak observed at 22.3° corresponds to quartz from the catalyst's supports used for the synthesis of the MWCNTs [23]. As depicted in Figure 1, the XRD diffraction pattern of rutile-TiO_2 indicates that the rutile mineral sample employed in this study consists majorly of the rutile (R) phase, though peaks corresponding to Anatase (A) phase, and Ilmenite (I) are also seen in agreement with Yilleng [19]. In the XRD patterns, diffraction peaks are observed at 27.4°, 36.17°, 54.34°, 56.6° and 61.58° corresponding to the rutile phase in agreement with standard peaks of rutile-TiO_2 in Joint Committee on Powder Diffraction Standards (JCPDS) file 47-0421 and 29-1360 [19]. These diffraction peaks correspond to the crystal planes of rutile (110), (101), (211), (220) and (002), respectively.

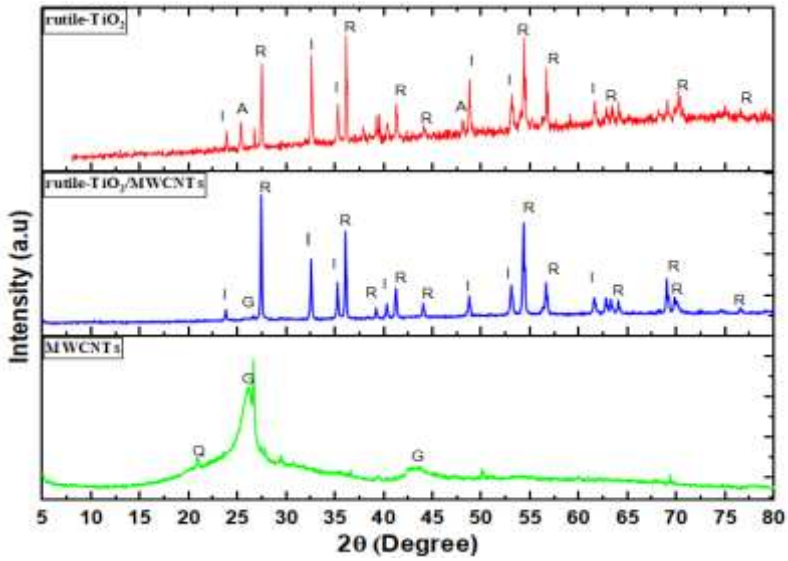

Figure 1: X-ray diffraction analysis (XRD) pattern of rutile-TiO_2, rutile-TiO_2/MWCNTs and MWCNTs

The XRD spectrum of rutile-TiO_2/MWCNTs nanocomposite shows that the incorporation of the MWCNTs on rutile-TiO_2 via the hydrothermal treatment altered the peaks intensity and sharpness as shown in Figure 1. The incorporation of MWCNTs into the rutile-TiO_2 via hydrothermal method resulted in enhanced peak intensity and sharpness, indicating a

higher degree of crystallinity compared to that of bare rutile-TiO_2. Also, there is the appearance of a new low diffraction peak at 2θ = 26.4° corresponding to 002 (d=3.3342 Å), suggesting that MWCNT was well incorporated into the matrix of the rutile-TiO_2. Additionally, the peaks corresponding to the anatase phase were not seen in the diffraction pattern of the composite catalyst, suggesting that the incorporation of MWCNTs on rutile-TiO_2 led to a phase shift from anatase to rutile phase. This result demonstrated that hydrothermal treatment is effective for the synthesis of the rutile-TiO_2/MWCNTs composite in agreement with the report of Shaban et al. [22]. The crystallite size of rutile-TiO_2 and rutile-TiO_2/MWCNTs nanocomposite was calculated using the Scherer formula [22] presented in (Equation 2):

$$d = \frac{k\lambda}{\beta cos\theta} \quad (2)$$

where k is a constant that depends on the crystallite shape (0.9, with the assumption of spherical particles), λ is the X-ray wavelength, β is the full width at half maximum of the selected peak and θ is the Bragg's angle of diffraction for the peak. The crystallite size of rutile-TiO_2 was calculated according to the peak width of the rutile phase at (2θ=36.17º) to be 34.4 nm and 30.74 nm for the rutile-TiO_2/MWCNTs nanocomposite, respectively. This result indicated that the incorporation of the MWCNTs in the matrix of rutile-TiO_2 reduced the crystal size by about 10.64%, further confirming that the developed composite has an improved property. This result is in agreement with the result of Shaari & Mohamed [17] who also reported a decrease in crystallite size after doping TiO_2 with Ce and CNT using the so-gel method. According to Kumar & Sellappa [21], the smaller the crystallite size, the better the photocatalytic performance of the photocatalyst. The improved performance displayed by the rutile-TiO_2/MWCNTs nanocomposite photocatalyst on the degradation of the pollutants considered in this study may be attributed to the enhanced crystallinity [28] and smaller particle size compared to the bare rutile-TiO_2.

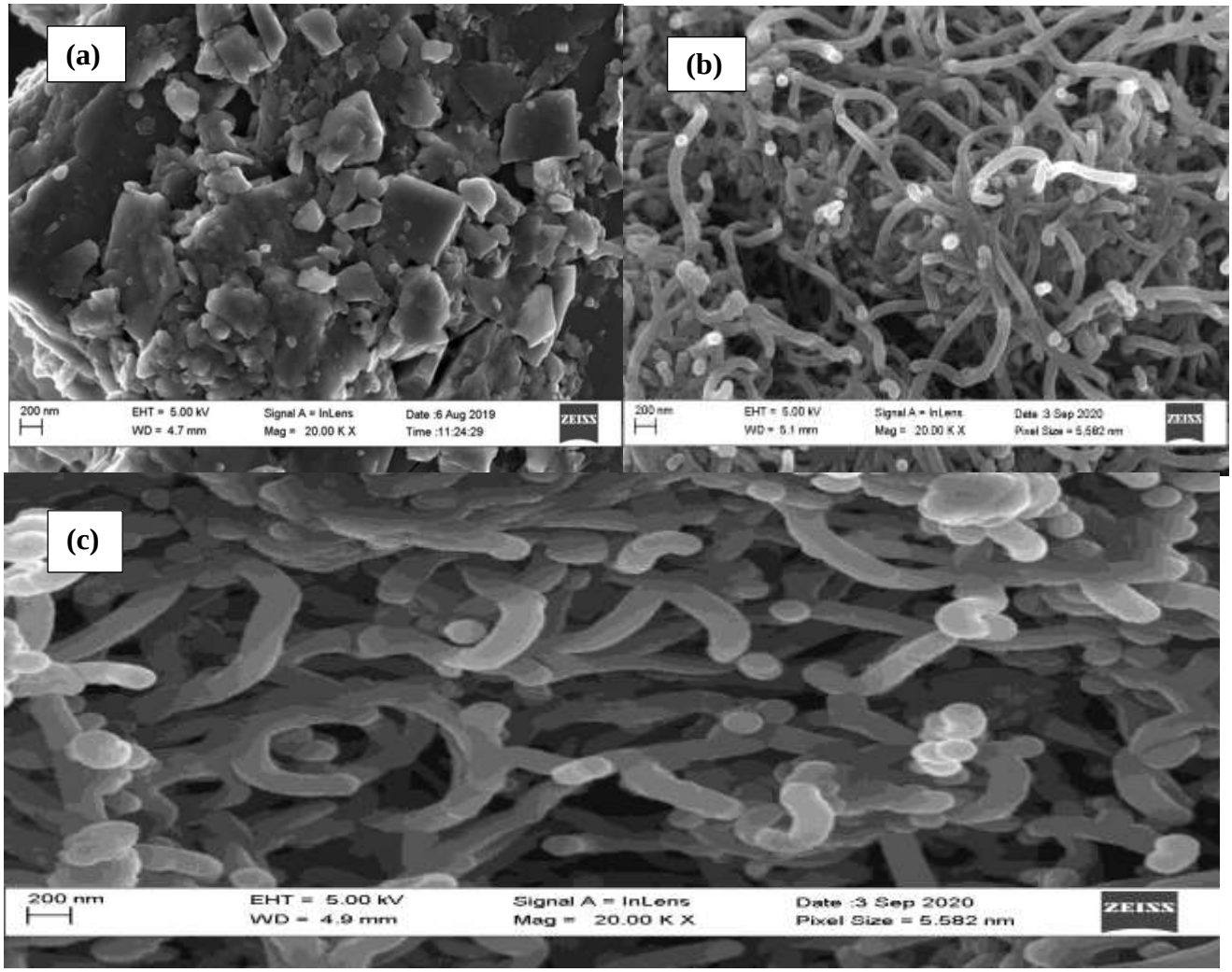

Figure 2: HRSEM micrographs of (a) rutile-TiO_2 (b) MWCNTs and (c) rutile-TiO_2/MWCNTs

3.1.2 HRSEM analysis of rutile-TiO_2, MWCNTs and rutile-TiO_2/MWCNTs nanocomposite

The surface morphology of rutile-TiO_2, MWCNTs, and TiO_2/MWCNTs nanocomposite were characterized by HRSEM. As presented in Figure 2a, it can be seen that the rutile-TiO_2 nanoparticles are composed primarily of closely packed

agglomerated irregularly shaped particles with no inter-particle gap contrary to the hexagonal shape reported by Yilleng [19]. The observed difference in the microstructure of rutile ore may be due to the difference in the location where the samples were collected. The HRSEM micrograph of MWCNTs (Figure 2b) shows aggregated long-length tube-like particles in agreement with previous reports [29,30]. Figure 2c reveals a less aggregated microstructure of MWCNTs intertwined TiO_2 nanoparticles. This result is similar to the report of Shaban et al. [22] for hydrothermal synthesis of TiO_2 Nanoribbons/Carbon nanotube composite from the hydrothermal route. The HRSEM image of rutile-TiO_2/MWCNTs corroborates the XRD results.

3.1.3 HRTEM analysis of MWCNTs and RutileTiO_2/MWCNTs nanocomposite

The microstructure and formation of the heterostructure between MWCNTs and TiO_2 were confirmed using HRTEM. Figures 3a and b depict the HRTEM Micrograph and SAED Pattern of MWCNTs, respectively while that of rutile-rutile-TiO_2/MWCNTs nanocomposite are presented in Figure 3c and d, respectively. The HRTEM image of MWCNTs reveals the formation of long tube-like particles, the dark spot seen in the HRTEM image of MWCNTs is due to the presence of catalyst support as earlier observed from the XRD result. The HRTEM image of rutile-TiO_2/MWCNT composites (Figure 3c) demonstrates that the aggregated particles of rutile-TiO_2 attached to the surface of the MWCNTs which confirmed the successful preparation of the rutile-TiO_2/MWCNTs nanocomposite through the hydrothermal route. This is in agreement with the report of Shaari & Mohamed [17]. The SAED pattern of both MWCNTs and rutile-TiO_2/MWCNTs nanocomposite shows the crystalline nature of both catalysts, the presence of sharp, bright diffraction ring spots in the SAED pattern of rutile-TiO_2/MWCNTs nanocomposite (Figure 3d) confirmed that the synthesized rutile-TiO_2/MWCNTs nanocomposite is more crystalline than MWCNTs in agreement with the report of Tijani et al., [11]. These findings indicate that the incorporation of MWCNTs with TiO_2 improved its crystallinity, and may be linked to the observed enhanced photocatalytic efficiency of the rutile-TiO_2/MWCNTs composite in agreement with Kumar and Sellappa [21].

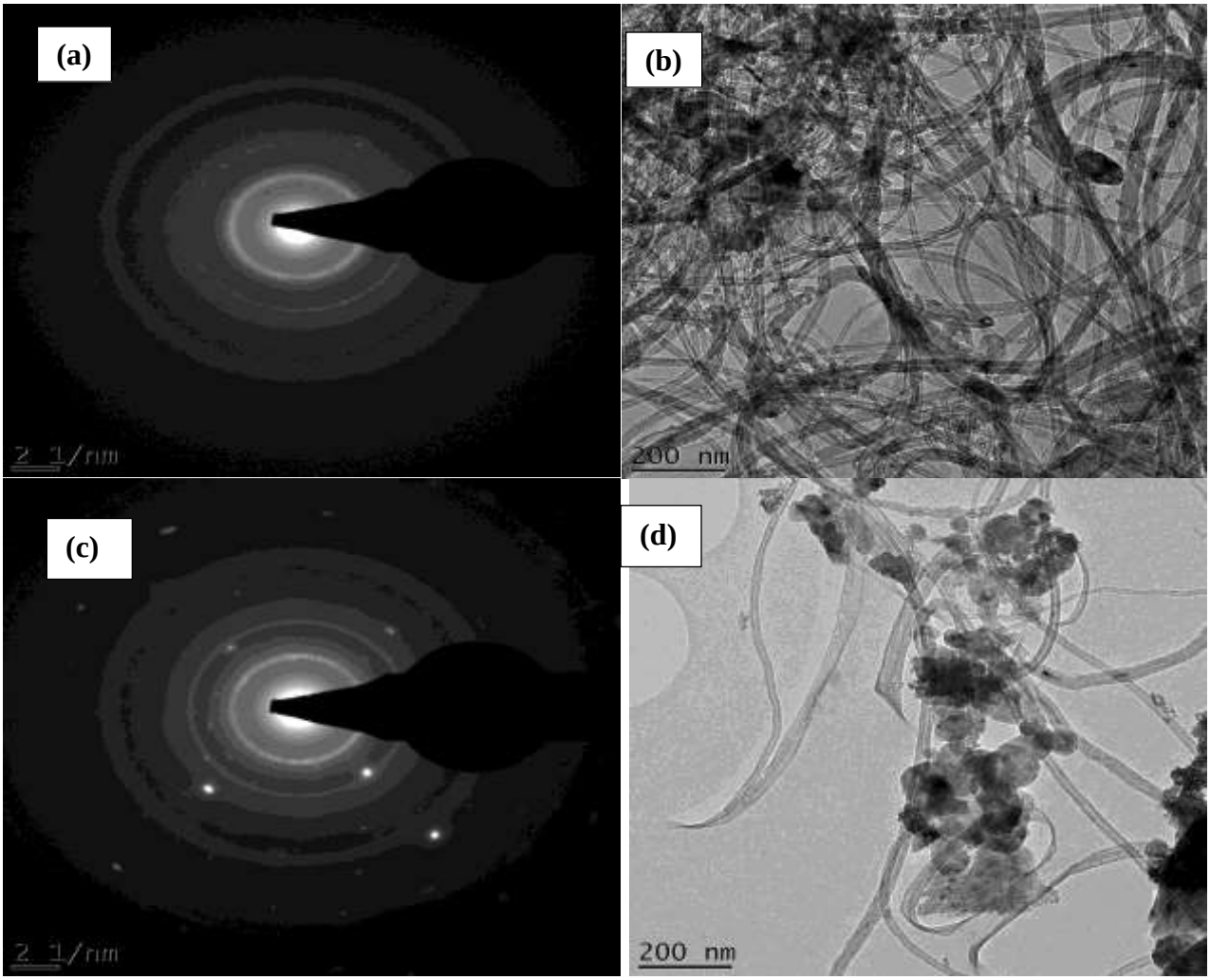

Figure 3: HRTEM Micrograph and SAED Pattern of (a and b) MWCNTs and (c and d) rutile-TiO2/MWCNTs nanocomposite

3.1.4 BET analysis of rutile-TiO_2, MWCNTs and rutile-TiO2/MWCNTs nanocomposite

The specific surface areas and the porosity of the rutile-TiO_2, MWCNTs, and rutile-TiO_2/MWCNTs nanocomposite were measured using BET analysis, and the results are presented in Table 1. The BET results show that the bare rutile-TiO_2 employed in this study possesses high surface area which is significantly higher compared to the value reported by Yilleng [19]. As presented in Table 1, the surface area of the synthesized rutile-TiO_2/MWCNTs nanocomposite is lower than that of bare rutile-TiO_2 contrary to the report of Shaari & Mohamed [17]; and Kumar & Sellappa [21]. This observation may be due to the incorporation of MWCNTs with rutile-TiO_2 as TiO_2 crystallites form clusters around the MWCNTs leading to the rutile crystallites of sizes bigger than that in bare rutile-TiO_2 and therefore reducing the surface area of the composite catalyst. This result is similar to the report of Xing et al. [31] for the surface area of TiO_2/activated carbon composite.

Table 1: BET analysis of rutile-TiO_2, MWCNTs and rutile-TiO_2/MWCNTs nanocomposite

Photocatalyst	Surface area[m^2/g]	Pore volume[cm^3/g]
TiO_2	921.1	0.453
MWCNTs	861.3	0.425
TiO_2/MWCNT	829.9	0.405

3.1.5 UV-vis analysis of rutile-TiO_2 and rutile-TiO_2/MWCNTs nanocomposite

UV-Vis absorption spectral analysis was carried out to determine the optical properties of the prepared rutile-TiO_2 and rutile-TiO_2/MWCNTs nanocomposite. The result (Figure not shown) reveals that the absorption of the rutile-TiO_2/MWCNTs photocatalyst extended largely towards visible light which started at a wavelength region of 264 nm, while the bare rutile-TiO_2 absorption region was at a wavelength of 221 nm. The extension of the absorption edge for rutile-TiO_2/MWCNTs to a longer wavelength suggested that TiO_2 and MWCNTs had good contact with each other. The addition of MWCNTs may enhance the light utilization efficiency because MWCNTs act as a light sensitizer, which injects the electrons into the conduction band of TiO_2 [21].

Reduction of the band gap of the photocatalyst is necessary to speed up the excitation of electrons from the valance band to the conducting band, thereby utilizing low energy which will provide more electron/positive hole pairs and enhance the photocatalytic removal of the pollutants. However, the removal process of pollutants is not controlled only by the value of band gap energy but also by the surface area, crystallinity, and density of adsorption active sites [12]

3.2.1 Photocatalytic performances of rutile-TiO_2 and rutile-TiO_2/MWCNTs nanocomposite

Before conducting the photocatalytic degradation of the textile wastewater, the raw textile wastewater was characterized to determine the level of selected physicochemical parameters using the established standard procedure, and the results obtained are presented in Table 2.

Table 2: Physicochemical assessment of the textile wastewater

Parameters	**Initial values**	**After treatment with**		**Permissible limit (World Health Organization, WHO 2012)**
		rutile-TiO_2	**rutile-TiO_2/MWCNTs**	
Ph	9.4	6.5	7.8	6-9
Odour	Offensive	Odourless	Odourless	
Colour	Bluish-green	Light Orange	Lighter Orange	
BOD(mg/l)	98	42	45	50
COD(mg/l)	400	240	120	<120
Phenol (mg/l)	0.99	0.4	0.2	0.25

The results of the selected physicochemical parameters reveal that the textile wastewater cannot be directly discharged into the environment without proper treatment as most parameters were above the WHO permissible limit. The discharge of wastewater containing phenol and its byproducts generates a significant risk to the aquatic environment [17]. Additionally, highly coloured wastewater containing dyes when discharged into the surrounding environment and water bodies are harmful to humans and animals by causing allergy, dermatitis, cancer, and skin irritation [22]. After the treatment, both rutile-TiO_2 and rutile-TiO_2/MWCNTs showed adequate photocatalytic performances with rutile-TiO_2/MWCNTs exhibiting the best photocatalytic performance, and most parameters were reduced to below the permissible limits. These results suggested that the rutile-TiO_2/MWCNTs nanocomposite developed in this study has the potential to be employed for the treatment of real textile wastewater before being discharged into the environment.

3.2.2 Effect of Time on the Degradation of Phenol and COD Textile in Wastewater

The photocatalytic performance was evaluated by the degradation of phenol and COD as the target pollutants. The photocatalytic performance of rutile-TiO_2 and rutile-TiO_2/MWCNTs nanocomposite were evaluated through their efficiency in the degradation of phenol under sunlight and artificial irradiation. The percentage removal of phenol under sunlight and artificial irradiation is shown in Figure 4. The degradation efficiency of rutile-TiO_2 and rutile-TiO_2/MWCNTs nanocomposite under light sources varies significantly due to several characteristics such as surface area, band gap energy,

and particle size. The degradation efficiency increases with an increase in time until equilibrium is attained and remains constant. Equilibrium was achieved in 150 min. As depicted in Figure 4a, the removal efficiency of rutile-TiO_2 for phenol degradation at equilibrium was 42.42% while that of the rutile-TiO_2/MWCNTs was 59.60% under artificial light irradiation, whereas under natural sunlight irradiation, significant phenol removal was observed; rutile-TiO_2 nanoparticles alone sequestered 56.57% phenol while, rutile-TiO_2/MWCNTs nanocomposite successfully removed 73.74% of phenol from textile wastewater under the same applied conditions. The removal efficiency obtained in this study under UV light irradiation using rutile-TiO_2 (rutile ore) is lower compared to the value reported by Yilleng et al. [19]. This may be as a result of competition for the photocatalyst active site from other pollutants present in the textile wastewater. The incorporation of MWCNTs in the rutile-TiO_2 matrix enhanced the photocatalytic degradation of phenol from textile wastewater in agreement with Shaari & Mohamed [17] & Azeez et al. [32]. A similar trend was observed for the degradation of COD. The percentage reduction of COD under sunlight and artificial irradiation is shown in Figure 5. The COD reduction was observed to be 35% for rutile-TiO_2 photocatalyst and 55% for rutileTiO_2/MWCNTs nanocomposite photocatalyst under artificial light irradiation at equilibrium, whereas under natural sunlight irradiation, significant COD reduction was observed; the percentage reduction of COD 40% and 70% on bare rutile-TiO_2 nanoparticles and rutile-TiO_2/MWCNTs nanocomposite, respectively under the same applied conditions. The enhanced photocatalytic performance of rutile-TiO_2/MWCNTs nanocomposite photocatalyst for degrading both COD and phenol may be ascribed to its improved characteristics such as crystallinity [18] as confirmed by the XRD results. Additionally, MWCNTs facilitate the narrowing of TiO_2 band gap and support electron transfer [21].

Also, both rutile-TiO_2 and rutile-TiO_2/MWCNTs nanocomposite photocatalysts on degradation of COD and phenol from real textile wastewater are higher under the natural sunlight compared to under the UV light probably due to the higher UV component in sunlight than in photo/visible light as observed by Tijani [11]. This result is also similar to the report of Martin et al. [33].

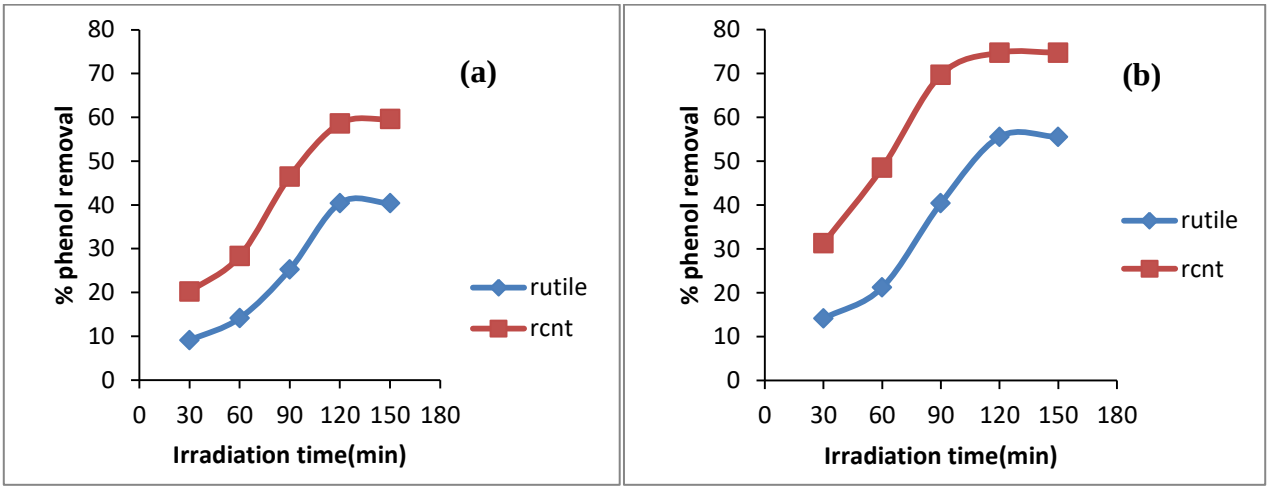

Figure 4: Phenol removal from textile wastewater under (a) UV light and (b) sunlight

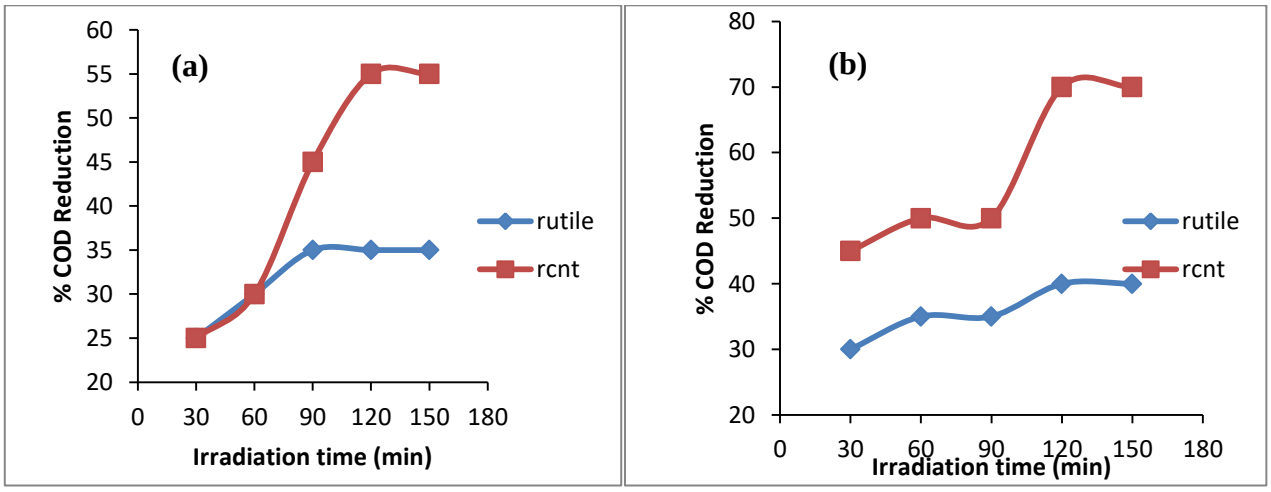

Figure 5: COD removal from textile wastewater under (a) UV and (b) sunlight

3.3 Degradation Kinetic

Pseudo-first-order and pseudo-second-order kinetic models were employed to assess the degradation behavior of phenol and COD using rutile-TiO_2 and rutile-TiO_2/MWCNTs nanocomposite. Equations of the studied kinetic models were expressed in (Equations 3 and 4) for the pseudo-first-order, and pseudo-second-order kinetic models, respectively [34].

$$ln\frac{C_o}{C_t} = k_{1App}t \quad (4)$$

$$\frac{1}{C_t} = \frac{1}{C_0} + k_{2App}t \quad (5)$$

where C_0 and C_t are the initial concentration and the concentration of phenol and COD after irradiation time (t); k_{1App} and k_{2App} are the apparent kinetic rate constants of pseudo-first-order and pseudo-second-order reaction kinetics, respectively; t is the reaction time. The pseudo-first-order kinetic model was investigated from the linear relation between ln (C_0/C_t) and t (Figures 6a and b) while the pseudo-second-order kinetic model was studied from the linear relation between $1/C_t$ and t (Figure 7a and b) for both phenol and COD. The kinetic parameters for these models are listed in Table 3.

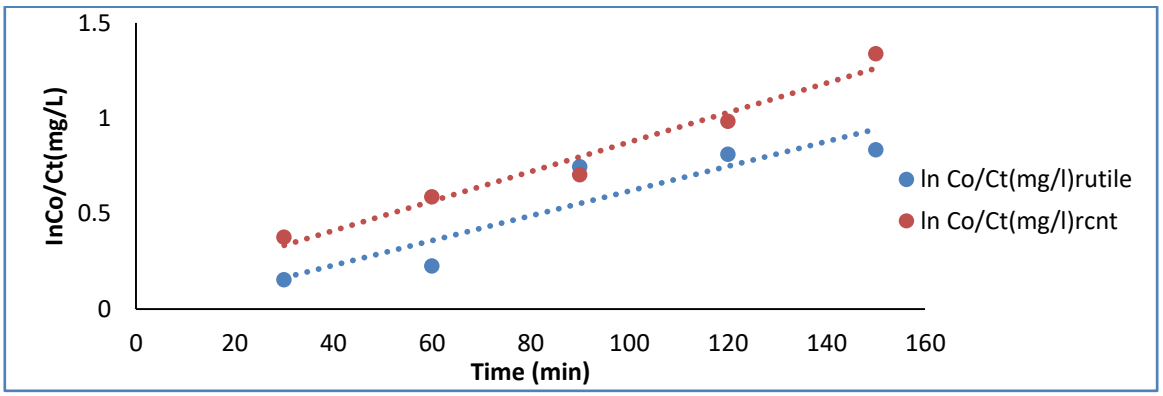

Figure 6a: Pseudo-first-order kinetic model for phenol degradation using rutile-TiO_2 and rutile-TiO_2/MWCNTs nanocomposite

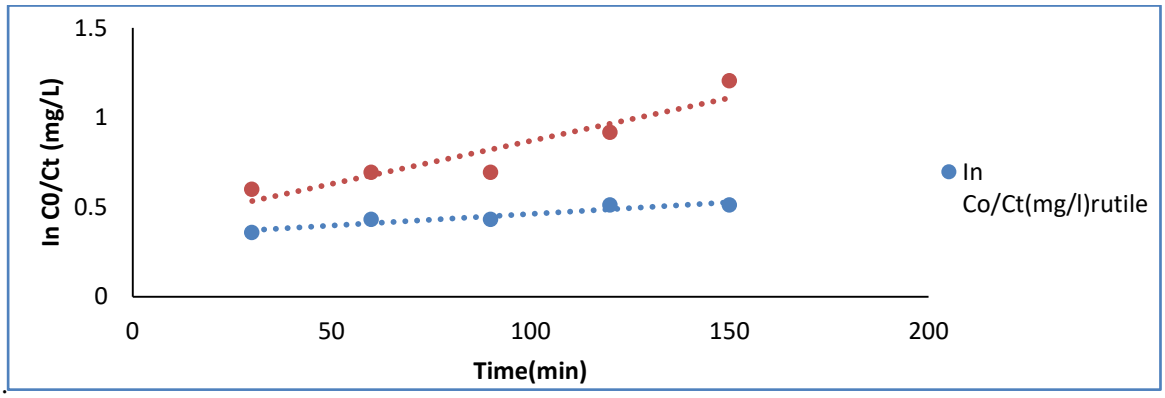

Figure 6b: Pseudo-first-order kinetic model for COD degradation using rutile-TiO_2 and rutile-TiO_2/MWCNTs nanocomposite.

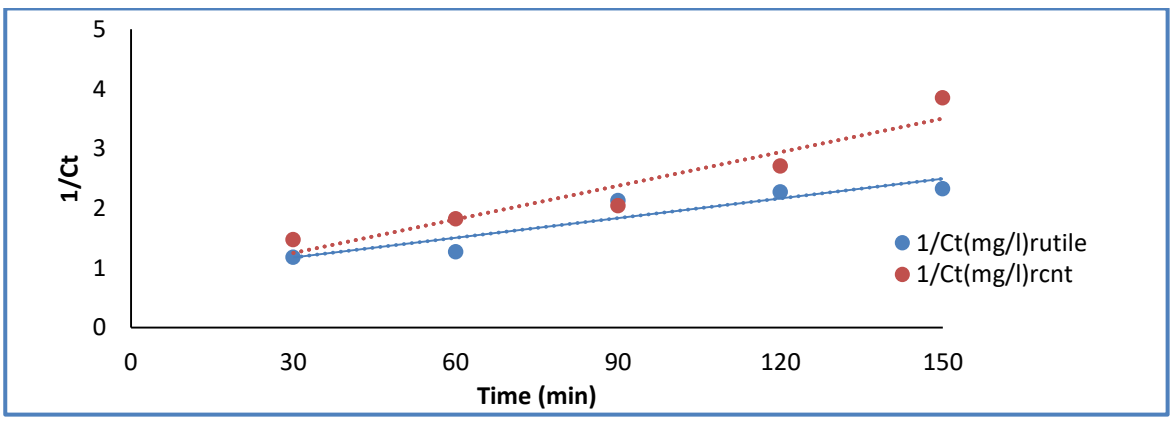

Figure 7a: Pseudo-second-order kinetic model for phenol degradation using rutile-TiO_2 and rutile-TiO_2/MWCNTs nanocomposite.

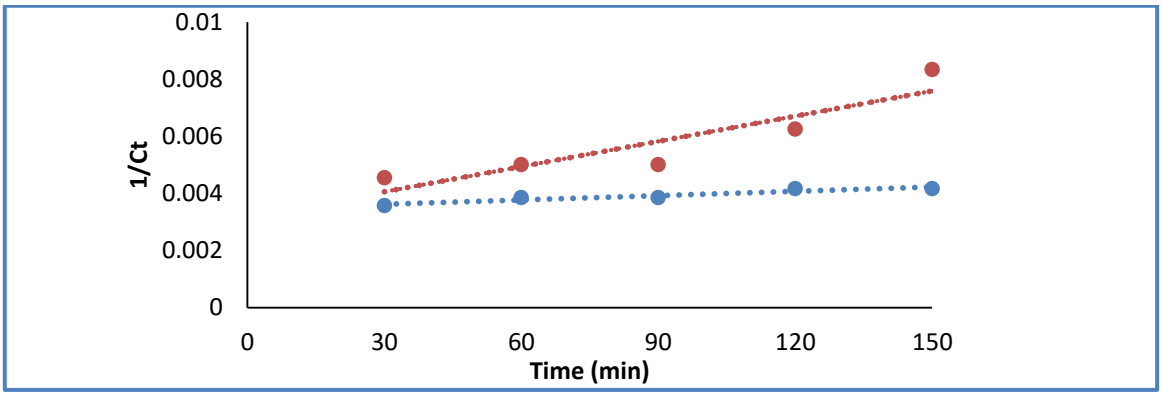

Figure 7b: Pseudo-second-order kinetic model for COD degradation using rutile-TiO_2 and rutile-TiO_2/MWCNTs nanocomposite

Table 3: Parameters of first and second-order kinetic models for phenol degradation using rutile-TiO_2 and rutile-TiO_2/MWCNT nanocomposites

Pollutants	Sample	Pseudo-first-order		Pseudo-second-order	
Phenol		k_{1App} (min^{-1})	R^2	k_{2App} ($M^{-1}min^{-1}$)	R^2
	rutile-TiO_2	0.0065	0.8430	0.0110	0.8564
	rutile-TiO_2/MWCNTs	0.0077	0.9660	0.0180	0.9045
COD					
	rutile-TiO_2	0.0013	0.8962	0.000005	0.8985
	rutile-TiO_2/MWCNTs	0.0048	0.8648	0.00003	0.8225

It can be seen from Table 3 that for both phenol and COD degradation, the pseudo-first-order gave the best coefficient of determination (R^2) for rutile-TiO_2 photocatalyst while the pseudo-second-order model gave the best for rutile-TiO_2/MWCNTs photocatalyst. The apparent rate constant determines the effectiveness of the photocatalysts, the estimated values of the apparent constants are considerably higher for rutile-TiO_2/MWCNTs nanocomposite photocatalyst in relation to that rutile-TiO_2 photocatalyst. This result further confirmed that the developed rutile-TiO_2/MWCNTs nanocomposite photocatalyst is more effective for degrading phenol and COD from textile wastewater. It is noteworthy that the values of the apparent rate constants for both bare rutile-TiO_2 and rutile-TiO_2/MWCNTs photocatalysts are higher for phenol than COD suggesting that the photocatalysts demonstrated more performance for phenol degradation.

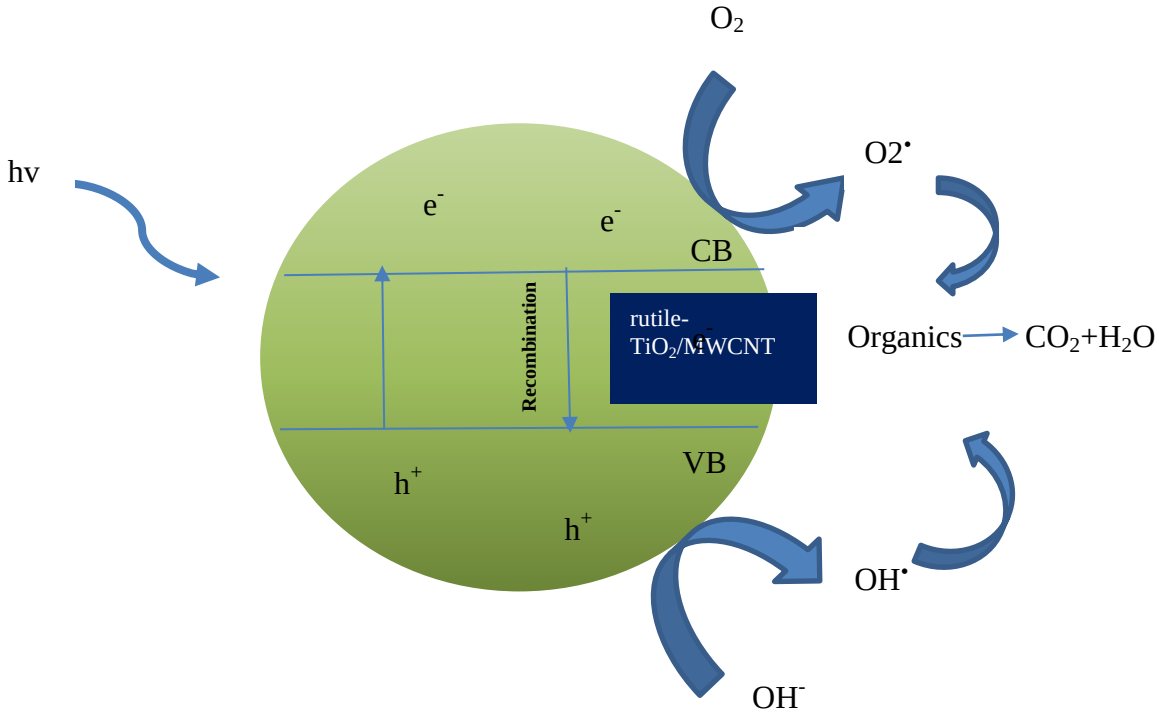

Figure 8: Mechanism of rutile-TiO_2 /MWCNTs nanocomposite for Phenol and COD Degradation

3.6 Possible Mechanism of Phenol and COD Degradation

As depicted in Figure 8, when rutile-TiO_2 absorbs photons under the natural sunlight, electrons are photoexcited from the valency band (CV) to the conduction band (CB) resulting in the formation of an electron-hole (e^-/h^+) pair. The electron transferred from rutile-TiO_2 to the surface absorbed oxygen O_2 to produce active oxygen species $O^{\bullet}$ which oxidizes to mineralise the pollutants (phenol and COD). The hole can react with OH^- or H_2O to produce hydroxyl radical $OH^{\bullet}$ which oxidizes the pollutants to CO_2 and H_2O. The MWCNTs incorporated on the matrix of rutile-TiO_2 /MWCNTs inhibit recombination rate by facilitating the electro transfer from rutile-TiO_2 thereby increasing the available electron for pollutants degradation.

4. CONCLUSION

In this study, a new kind of rutile-TiO_2/MWCNTs nanocomposite photocatalyst was successfully produced through a hydrothermal process. The XRD, HRSEM, and HRSEMTEM analysis confirmed the formation of crystalline rutile-TiO_2/MWCNTs nanocomposite. The degradation of textile wastewater under artificial and natural solar irradiation was used to test the photocatalytic performance of the produced rutile-TiO_2 and rutile-TiO_2/MWCNTs nanocomposite. The photocatalytic performance was evaluated by the degradation of phenol and COD as the target pollutants. Photocatalytic results showed equilibrium was achieved at 150 min and that the synthesised rutile-TiO_2/MWCNTs nanocomposite showed a better performance both under UV and sunlight irradiation than onto bare rutile-TiO_2; Under UV light, the removal phenol onto pure rutile-TiO_2 and rutile-TiO_2/MWCNTs was 42% and 59%, respectively while under the sunlight it was 56% and 73%, respectively at equilibrium. Similarly, the percentage reduction of COD under visible light is 35% and 55% onto rutile alone and rutile-TiO_2/MWCNTs, respectively whereas, under sunlight, it was 40% and 70%, onto bare rutile-TiO_2 and rutile-TiO_2/MWCNTs, respectively at equilibrium. The synthesised rutile-TiO_2/MWCNTs composite has been demonstrated to be a potential effective photocatalyst for the degradation of textile wastewater and may be explored for the treatment of other industrial effluents.

ACKNOWLEDGEMENT

The authors wish to acknowledge the Chemical Engineering Department, University of Ilorin, Nigeria, and the Africa Centre of Excellence for Mycotoxin & Food Safety, Federal University of Technology, Nigeria, for granting us permission to use the laboratory facilities.

REFERENCES

[1] Huo, H., Hu, X., Wang, H., Li, J., Xie, G., Tan, X., & Jin, Q. (2019). Synergy of Photocatalysis and Adsorption for Simultaneous Removal of Hexavalent Chromium and Methylene Blue by g-C $_3$ N_4 / $BiFeO_3$ / Carbon Nanotubes Ternary Composites. *International Journal of Environmental Research and Public Health*, *16*(17), 3219.

[2] Crini, G., Lichtfouse, E., Wilson, L. D., & Morin-Crini, N. (2019). Conventional and non-conventional adsorbents for wastewater treatment. *Environmental Chemistry Letters*, *17*, 195-213.

[3] Awogbemi, O., & Von Kallon, D. V. (2023). Progress in agricultural waste derived biochar as adsorbents for wastewater treatment. *Applied Surface Science Advances*, *18*, 100518

[4] Abbas, A., Al-Amer, A. M., Laoui, T., Al-Marri, M. J., Nasser, M. S., Khraisheh, M.& Atieh M. A. (2016). Heavy metal removal from aqueous solution by advanced carbon nanotubes: a critical review of adsorption applications. *Separation and Purification Technology*, 157, 141–161.

[5] Singh, R. P., Singh, P. K., Gupta, R., & Singh, R. L. (2019). Treatment and recycling of wastewater from textile industry. *Advances in biological treatment of industrial waste water and their recycling for a sustainable future*, 225-266.

[6] Li, J., Cao, Y., Ding, K., Ye, J., Li, F., Ma, C., Lv, P., Xu Y. & Shi, L. (2024). Research progress of industrial wastewater treatment technology based on solar interfacial adsorption coupled evaporation process. *Science of The Total Environment*, 172887.

[7] Leal Filho, W., Ellams, D., Han, S., Tyler, D., Boiten, V. J., Paço, A., Moora, H. & Balogun, A.-L. (2019). A review of the socio-economic advantages of textile recycling. *Journal of cleaner production*, *218*, 10-20.

[8] Fatiha, M., & Belkacem, B. (2015). Adsorption of methylene blue from aqueous solutions using Fe_3O_4/ bentonite nanocomposite. *J. Mater. Environ. Sci*, *7*(1), 285–292.

[9] Khan, S., Noor, A., Khan, I., Muhammad, M., Sadiq, M., & Muhammad, N. (2022). Photocatalytic degradation of organic dyes contaminated aqueous solution using binary $CdTiO_2$ and ternary $NiCdTiO_2$ nanocomposites. *Catalysts*, *13*(1), 44.

[10] Adesina, O. A., Taiwo, A. E., Akindele, O., & Igbafe, A. (2021). Process parametric studies for decolouration of dye from local 'tie and dye'industrial effluent using Moringa oleifera seed. *South African Journal of Chemical Engineering*, *37*, 23-30.

[11] Tijani, J. O., Momoh, U. O., Salau, R. B., Bankole, M. T., Abdulkareem, A. S., & Roos, W. D. (2019). Synthesis and characterization of $Ag_2O/B_2O_3/TiO_2$ ternary nanocomposites for photocatalytic mineralization of local dyeing wastewater under artificial and natural sunlight irradiation. *Environmental Science and Pollution Research*, *26*(19), 19942–19967.

[12] Khan, S., Noor, T., Iqbal, N., & Yaqoob, L. (2024). Photocatalytic Dye Degradation from Textile Wastewater: A Review. *ACS omega*, 2024 (9) 21751-21767

[13] Rashed, M. N., Eltaher, M. A., & Abdou, A. N. A. (2017). Subject Category : Subject Areas : Adsorption and photocatalysis for methyl orange and Cd removal from wastewater using TiO_2 / sewage sludge-based activated carbon nanocomposites. Royal Society open science 4: 170834
[14] Wang, X., Jiang, J., & Gao, W. (2022). Reviewing textile wastewater produced by industries: characteristics, environmental impacts, and treatment strategies. *Water Science and Technology*, *85*(7), 2076-2096.
[15] Khan, M. M. (2021). Principles and mechanisms of photocatalysis *Photocatalytic systems by design* 1-22: Elsevier
[16] Lawal, A., Muhammad, Z., Obunadike, C., Yakubu, Y., Ogunsanmi, A., Abdulrazak, O., Ayodele, C. O. & Komolafe, F. (2022). Photocatalytic Degradation of Phenol in Wastewater: A Mini Review. *International Journal of Research and Innovation in Applied Science*, *7*(9), 59-64.
[17] Shaari, N., Tan, S. H., & Mohamed, A. R. (2012). Synthesis and characterization of CNT / Ce-TiO2 nanocomposite for phenol degradation Synthesis and characterization of CNT / Ce-TiO 2 nanocomposite for phenol degradation. *Journal of Rare Earths*, *30*(7), 651–658.
[18] Heydari, Z., & Ghadam, P. (2023). Biosynthesis of Titanium Dioxide Nanoparticles by the Aqueous Extract of Juglans regia Green Husk. *Materials Proceedings*, *14*(1), 43.
[19] Yilleng, M. T., Gimba, E. C., Ndukwe, G. I., & Bugaje, I. M. (2015). Assessing the Photo Catalytic Activity of Rutile Ore from the Middle Belt Region of Nigeria on the Degradation of Phenol in Water. *Journal of Applied Chemistry (IOSR-JAC)*, *8*(7), 36–43.
[20] Kumar, A., & Gajanan, P. (2018). Comparative Photocatalytic Degradation of Rose Bengal Dye under Visible Light by TiO2, TiO2/PAni and TiO2/PAni/GO Nanocomposites. *International Journal for Research in Applied Science and Engineering Technology*, *6*(2), 339–350.
[21] Kumar, D. S., & Sellappa, K. (2019). Photocatalytic Degradation Of Reactive Dyes And Real Textile Composite Wastewater Using Tio2/Mwcnt Nanocomposite Under Uva And Uva-Led Irradiation. A Comparative Study. *Environment Protection Engineering*, *45*(2), 95-116.
[22] Shaban, M., Ashraf, A. M., & Abukhadra, M. R. (2018). TiO_2 nanoribbons/carbon nanotubes composite with enhanced photocatalytic activity; fabrication, characterization, and application. *Scientific reports*, *8*(1), 1-17.
[23] Adewoye, T., Ogunleye, O., Abdulkareem, A., Salawudeen, T., & Tijani, J. (2021). Optimization of the adsorption of total organic carbon from produced water using functionalized multi-walled carbon nanotubes. *Heliyon*, *7*(1), e05866.
[24] Akbaba, U. (2019). Effect of Different Acid Components on Multi-Walled Carbon Nanotubes. *Hittite Journal of Science and Engineering*, *6*(4), 319-323.
[25] Kurc, B., Siwińska-Stefańska, K., Jakóbczyk, P., & Jesionowski, T. (2016). Titanium dioxide/graphene oxide composite and its application as an anode material in non-flammable electrolyte based on ionic liquid and sulfolane. *Journal of Solid State Electrochemistry*, *20*, 1971-1981
[26] Eswaran, P., Madasamy, P. D., Pillay, K., & Brink, H. (2024). Sunlight-driven photocatalytic degradation of methylene blue using ZnO/biochar nanocomposite derived from banana peels. Biomass Conversion and Biorefinery, 1-21.
[27] Taha, W. M., Morsy, M., Nada, N. A., & Ibrahim, M. A. (2022). Preparation and Characterization of Multiwall Carbon Nanotubes Decorated with Copper Oxide. *Egyptian Journal of Chemistry*, *65*(7), 305-312.
[28] Permana, M. D., Noviyanti, A. R., Lestari, P. R., Kumada, N., Eddy, D. R., & Rahayu, I. (2022). Synthesis and photocatalytic activity of TiO2 on phenol degradation. *Kuwait Journal of Science*, *49*(4), 1-13.
[29] Bankole, M. T., Mohammed, I. A., Abdulkareem, A. S., Tijani, J. O., Ochigbo, S. S., Abubakre, O. K., & Afolabi, A. S. (2018). Optimization of supported bimetallic (Fe-Co/CaCO3) catalyst synthesis parameters for carbon nanotubes growth using factorial experimental design. *Journal of Alloys and compounds*, *749*, 85-102.
[30] Hiremath, P., Ranjan, R., DeSouza, V., Bhat, R., Patil, S., Maddodi, B., Shivamurthy B., Perez T. C. & Naik, N. (2023). Enhanced wear resistance in carbon nanotube-filled bio-epoxy composites: a comprehensive analysis via scanning electron microscopy and atomic force microscopy. *Journal of Composites Science*, *7*(11), 478.
[31] Xing, B., Shi, C., Zhang, C., Yi, G., Chen, L., Guo, H., Huang G. & Cao, J. (2016). Preparation of TiO_2/activated carbon composites for photocatalytic degradation of RhB under UV light irradiation. *Journal of nanomaterials*, *2016*(1), 8393648.
[32] Azeez, S. O., Saheed, I. O., Adekola, F. A., & Salau, S. S. (2022). Preparation of TiO2-activated kaolinite composite for photocatalytic degradation of rhodamine B dye. *Bulletin of the Chemical Society of Ethiopia*, *36*(1), 13-24.
[33] Martin, M. V., Ipiña, A., Villabrille, P. I., & Rosso, J. A. (2017). Combination of sunlight, oxidants, and Ce-doped TiO 2 for phenol degradation. *Environmental Science and Pollution Research*, *24*, 6013-6021.
[34] Asefa, G., Negussa, D., Lemessa, G., Alemu, T. & Nanomater J. (2024) The Study of Photocatalytic Degradation Kinetics and Mechanism of Malachite Green Dye on Ni–TiO2 Surface Modified with Polyaniline. Journal of Nanomaterials 2024 (1) 5259089.